Simulating A Self-propelled Submerged Body in a Coastal Ocean Hindcast Using the NRL-MIT Nonhydrostatic Model

Dr. Patrick C. Gallacher
Naval Research Laboratory, Ocean Sciences Branch
Stennis Space Center, MS 39529
phone: (228) 688-5315; fax: (228) 688-4149; e-mail: gallacher@nrlssc.navy.mil

Dr. David A. Hebert
National Research Council Postdoctoral Fellow
Naval Research Laboratory, Ocean Sciences Branch
Stennis Space Center, MS 39529

Award Number: N0001408WX20173, N0001408WX20544, N0001408WX20181

LONG-TERM GOALS

- To enhance our ability to detect self-propelled submerged bodies (SSBs), e.g. submarines and AUVs at a distance. Little work has been done to improve our understanding of how we can sense changes in the environment caused by internal waves (IWs) and wakes generated by the passage of an SSB.

Simulations of self-propelled submerged bodies have been conducted in idealized environments with simple environmental geometries and stratifications. The focus of those simulations was on improving the submarine, i.e. reduced drag, less vortex production, improved maneuverability and greater speed. Thus many of the simulations focused on the near field and on complex, realistic submarine geometry. Some simulations looked at the far field but usually for simple shapes and simple background stratification.

OBJECTIVES

- To incorporate the ability to simulate a SSB into the NRL-MIT nonhydrostatic model. A SSB can be simulated as a smooth, bluff or streamlined body moving through the model domain. It can also be simulated as a point momentum source with or without swirl (to better simulate a propeller) to generate the extreme far field.

These simulations will focus on the environmental impact of a SSB to improve our understanding of the signatures that would be measured by acoustical or E+M systems. To this end we are interested in hindcasting realistic coastal ocean environments with accurate stratification, currents, ambient IW fields and bathymetry and simulating changes in this environment caused by the wake and IWs generated by the SSBs movement. In a stratified fluid the wake collapses vertically and spreads horizontally. Thus its signature becomes very two dimensional. However, the collapse also generates IWs which propagate three dimensionally thus yielding additional potential signatures of the SSB.

Report Documentation Page

Form Approved
OMB No. 0704-0188

Public reporting burden for the collection of information is estimated to average 1 hour per response, including the time for reviewing instructions, searching existing data sources, gathering and maintaining the data needed, and completing and reviewing the collection of information. Send comments regarding this burden estimate or any other aspect of this collection of information, including suggestions for reducing this burden, to Washington Headquarters Services, Directorate for Information Operations and Reports, 1215 Jefferson Davis Highway, Suite 1204, Arlington VA 22202-4302. Respondents should be aware that notwithstanding any other provision of law, no person shall be subject to a penalty for failing to comply with a collection of information if it does not display a currently valid OMB control number.

1. REPORT DATE	2. REPORT TYPE	3. DATES COVERED
30 SEP 2008	**Annual**	**00-00-2008 to 00-00-2008**

4. TITLE AND SUBTITLE	5a. CONTRACT NUMBER
Simulating A Self-Propelled Submerged Body In A Coastal Ocean Hindcast Using The NRL-MIT Nonhydrostatic Model	5b. GRANT NUMBER
	5c. PROGRAM ELEMENT NUMBER
6. AUTHOR(S)	5d. PROJECT NUMBER
	5e. TASK NUMBER
	5f. WORK UNIT NUMBER
7. PERFORMING ORGANIZATION NAME(S) AND ADDRESS(ES) **Naval Research Laboratory, Ocean Sciences Branch,Stennis Space Center,MS,39529**	8. PERFORMING ORGANIZATION REPORT NUMBER
9. SPONSORING/MONITORING AGENCY NAME(S) AND ADDRESS(ES)	10. SPONSOR/MONITOR'S ACRONYM(S)
	11. SPONSOR/MONITOR'S REPORT NUMBER(S)

12. DISTRIBUTION/AVAILABILITY STATEMENT
Approved for public release; distribution unlimited

13. SUPPLEMENTARY NOTES
code 1 only

14. ABSTRACT
To enhance our ability to detect self-propelled submerged bodies (SSBs), e.g. submarines and AUVs at a distance. Little work has been done to improve our understanding of how we can sense changes in the environment caused by internal waves (IWs) and wakes generated by the passage of an SSB.

15. SUBJECT TERMS

16. SECURITY CLASSIFICATION OF:			17. LIMITATION OF ABSTRACT	18. NUMBER OF PAGES	19a. NAME OF RESPONSIBLE PERSON
a. REPORT	b. ABSTRACT	c. THIS PAGE			
unclassified	**unclassified**	**unclassified**	**Same as Report (SAR)**	**12**	

APPROACH

A relatively smooth object can be inserted into the NRL-MIT model using the immersed boundary method (IMB). Several versions of this technique have been developed e.g. Tseng and Ferziger (2003), Goldstein et al. (1993), Lai and Perskin (2000), and Fadlun et al. (2000). Tseng and Ferziger demonstrated their version by using it to simulate a complex bottom bathymetry in the MIT model.

The submerged body must be self-propelled because there are significant differences between towed (drag) wakes and self-propelled (momentumless) wakes. The details of the geometries and relative motions of the parts of the SSB, e.g. sail, diving planes, and propeller(s) or jet, are critically important in determining the near wake. However, much of the detail is lost in the far wakes particularly after wake collapse at approximately 7Nt (where N is the Brunt-Vaisala frequency). However, swirl from the propulsion system can remain a factor for many nondimensional time periods.

We plan to simulate the SSB as a smooth, self-propelled body with and without swirl. Since we are interested in the far wake and the IW fields that are generated from the wake, particularly during wake collapse, we are not concerned about the details of the SSBs geometry. Also for larger domains and coarser resolution we can simulate the SSB using a subgrid scale (SGS) model. The SGS model includes the SSB as a point source of momentum, e.g. Sirviente and Patel (1997) . By using the SGS model as a lateral BC we can extend the simulation results to regions remote from the SSB.

WORK COMPLETED

Scaling analysis and an examination of the limitations on computational domain size led us to parameterize the submarine as a momentum source (i.e., a jet) at the simulation boundary. Attempting to simulate the submarine as a body of finite size would have restricted us to a domain too close to the submarine. We are interested in the mid-range to far field jet of the submarine and its interactions with the ambient internal wave field.

We first simulated a jet in an unstratified, homogeneous fluid. The results were compared with analytically derived similarity profiles and laboratory data. We then simulated a jet in linearly stratified fluid. The ratio of vertical to horizontal kinetic energy was calculated for several stratifications. The results were similar to those found in numerous laboratory experiments and other numerical experiments.

Finally, we have started inserting a jet into a realistic simulation of the ambient temperature, salinity and velocity in the vicinity of the Alabama Alps in the Gulf of Mexico (GoM). This simulation includes full Alabama Alps bathymetry and is initialized with observed temperature and salinity profiles. The Alabama Alps significantly affect the flow in their vicinity. The flow over the Alps generates hydraulic jumps, trapped lee waves, large amplitude internal waves and vortices that propagate downstream. Also, temperature and salinity are mixed and turbulent boundary layers form behind the alps for the higher velocity flows.

RESULTS

HOMOGENEOUS FLUID

The first experiments involved a round axisymmetric jet flowing into a homogeneous fluid. The parameters for this experiment are given in Table 1.

Table 1: Parameters used in homogeneous jet simulations.

L_x (m)	L_y(m)	L_z(m)	Δx(m)	Δy(m)	Δz(m)	U_0 (m/s)	D (m)	Δt (s)
480	160	160	1	1	1	0.2	10	1

Using U_0 and D as velocity and length scales, the Reynolds number is defined as:

$$\mathrm{Re}_D = \frac{U_0 D}{\nu} \tag{1}$$

In this study two Reynolds number simulations are performed, Re_D=400 and Re_D =2000. Figure 1 contains horizontal and vertical cross-sections of the flow evolution for each Re_D at t=10800s. The Re_D =400 simulation appears to be laminar with a nicely formed vortex pair at the jet leading edge. In contrast, the Re_D =2000 simulation appears to be turbulent, spreading faster and traveling slower downstream than the laminar jet. The turbulent jet has larger velocity gradients than laminar flow, resulting in a higher rate of energy dissipation and ambient fluid entrainment.

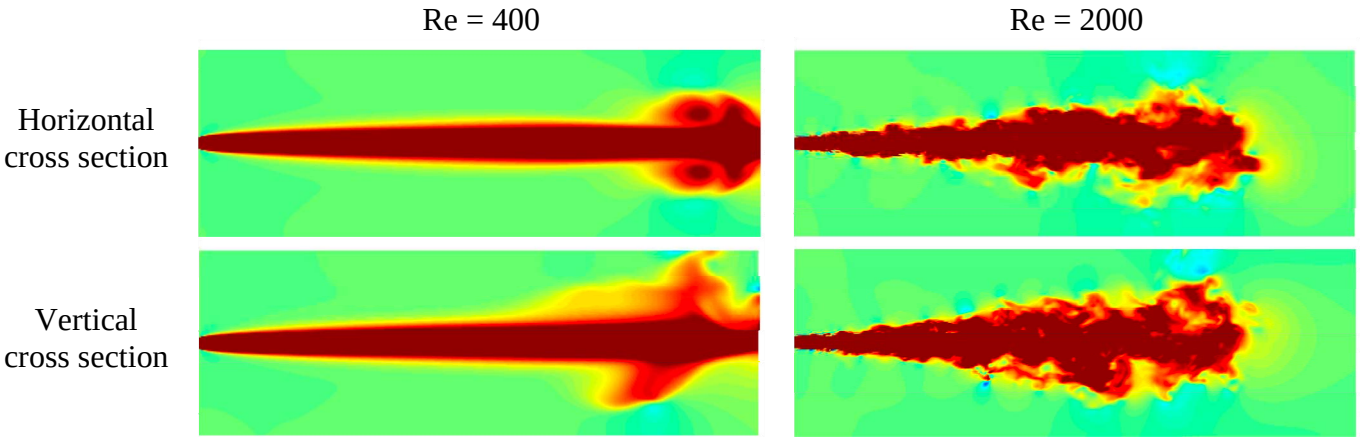

Figure 1. (Upper) Horizontal and (lower) vertical cross-section of U for each Re. Both plots are at t = 10800s. The Re_D=400 jet is laminar with a vortex pair formed at the leading edge of the jet. The Re_D=2000 jet is turbulent with large velocity gradients seen. Due to large velocity gradients the turbulent jet dissipates more energy than the laminar jet and does not extend into the domain as quickly as the laminar jet.

As each jet progresses downstream the initial top-hat jet becomes Gaussian in shape. Analytic results (e.g., Pope 2000, Tennekes and Lumley 1972) demonstrate that the jet will become Gaussian and will be self-similar when scaled by the centerline velocity, U_c, and jet half width, $r_{½}$. The scaled velocity profiles are shown in Figure 2, and fit well to a Gaussian curve after x/D=10. The profiles are the result of averaging over 50 snapshots of the model. The turbulent profiles do not fit the Gaussian as well as the laminar jet, possibly because the averaging period was too short to minimize turbulent fluctuations.

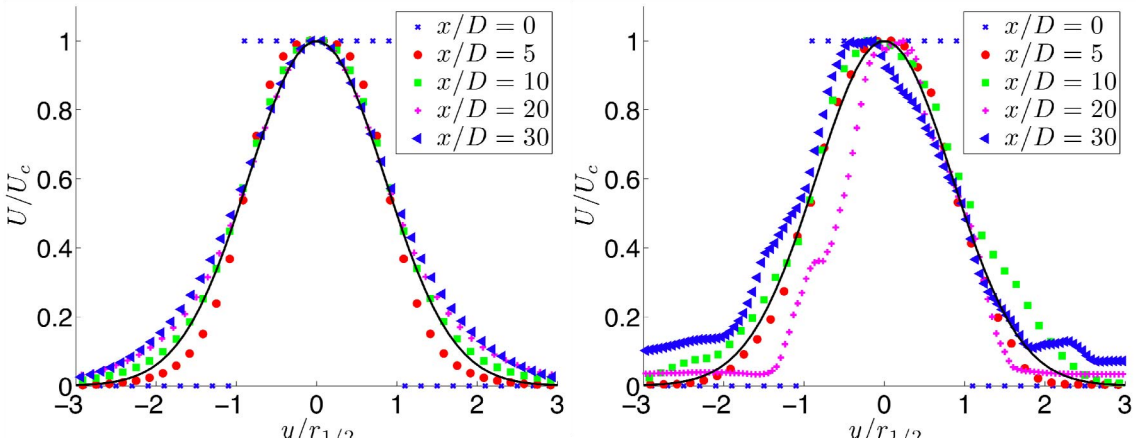

Figure 2. Normalized horizontal (xy) plane profiles of U for Re_D=400 (left) and Re_D=2000 (right). A top hat shape is seen at the jet origin x/D=0. The profiles become self similar (solid black line) by x/D=5 when scaled by centerline velocity, U_c, and jet half width, $r_{½}$. Noise in the Re_D=2000 jet may be a result of turbulent fluctuations that have not been removed via ensemble averaging.

LINEARLY STRATIFIED FLUID

In the second set of simulations the jet flows into a linearly stratified fluid. In stratified flows buoyancy forces exist that can affect the flow. The Froude number is now defined, which is the ratio of inertial to buoyancy forces:

$$F = \frac{U_0}{ND}, \tag{2}$$

where $N = \frac{g}{\rho_0}\frac{d\rho}{dz}$ is the buoyancy frequency and is a measure of the "strength" of the density stratification. Stratification inhibits the vertical spreading of the jet due to the buoyancy forces (Figure 3), and the jet becomes asymmetric compared to the jet in homogeneous fluid. For F=1 the outer jet edge is wavy and demonstrates alternating positive and negative x-direction flow suggesting a weak von Kärman vortex street has formed.

The vertical extent of the jet does not increase with decreasing Froude number as anticipated. This might be explained by the relative short time of the simulation whereby any noticeable vertical difference have not formed yet or it may be an artifact of the contouring. The impact of stratification can be seen, however, in plots of the volume averaged horizontal, $\langle E_H \rangle$, and vertical, $\langle E_V \rangle$, kinetic energy (Figure 4). As expected, the vertical kinetic energy decreases and the horizontal kinetic energy increases with decreasing Froude number, increasing stratification. This result is in agreement with analytical studies (e.g., Lilly 1983) and numerical experiments (e.g., Riley and de Bruyn Kops 2003).

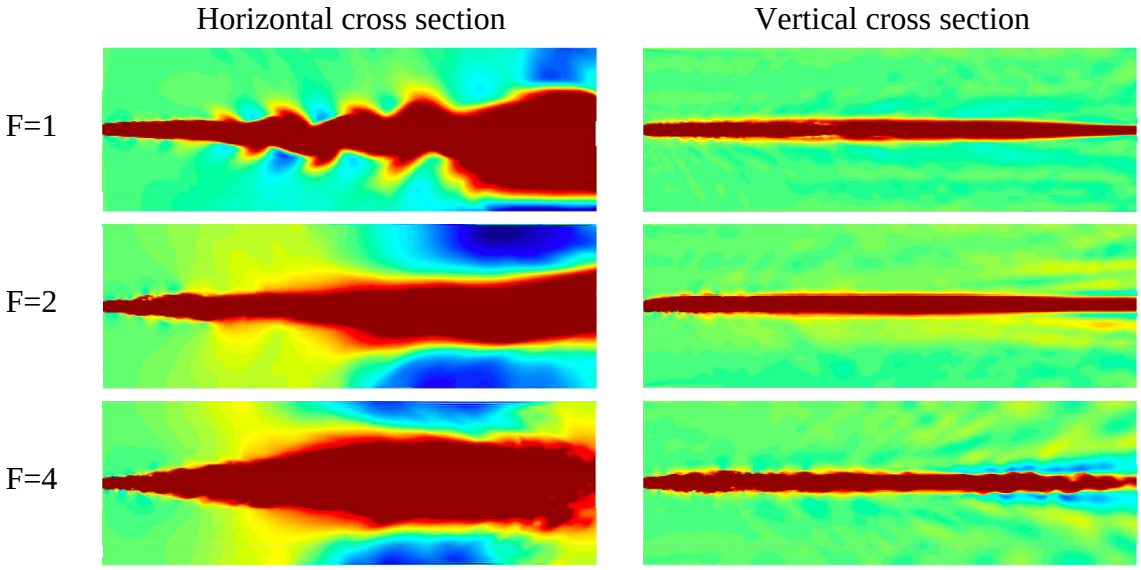

Figure 3. (Left) Horizontal and (Right) Vertical slices of U for F=1,2,4, Re_D=2000, t=10800s. The horizontal cross section shows a wavy pattern with oscillating velocity for the strongly stratified F=1 case, reminiscent of a vortex street. There is not noticeable different in the vertical heights of each jet. This is likely a result of the jet not having enough time to fully develop.

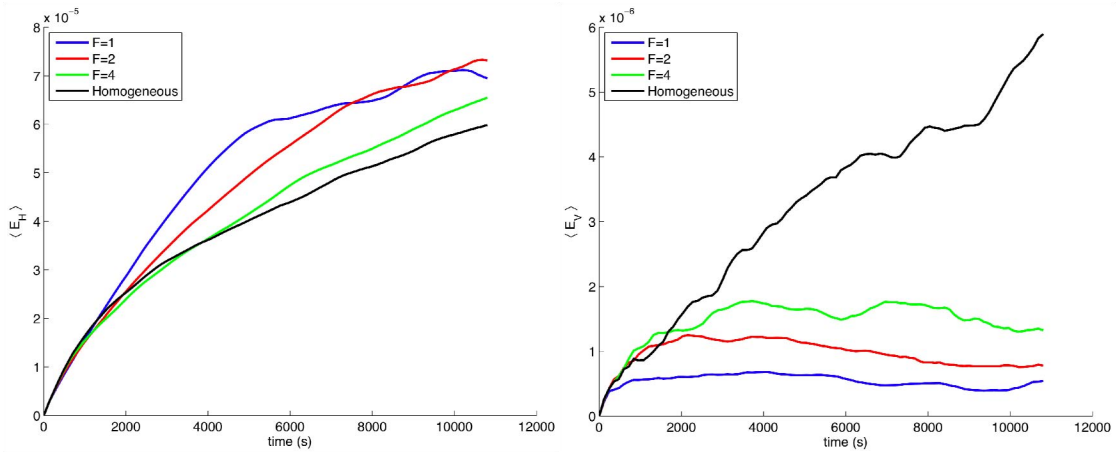

Figure 4. Evolution of $\langle E_H \rangle$ (left) and $\langle E_V \rangle$ (right) for each Froude number and Re=2000. The homogeneous flow is plotted as a black line for comparison. A clear trend is seen where as the stratification becomes stronger (i.e., F decreases), the jet decays slower and has reduced vertical kinetic energy. This indicates the flow becomes less 3D (or more 2D) with increased stratification and vertical decoupling of the flow, in agreement with theoretical (e.g., Lilly 1983) and numerical studies (e.g., Riley and de Bruyn Kops, 2003).

REALISTIC STRATIFICATION/SIMULATIONS IN THE GULF OF MEXICO

The motivation for the work in this section is to simulate the wake of a submarine near variable topography and in realistically stratified water. The Alabama Alps, which is a submerged ridge in the GoM, were chosen. Common to all simulations in this section are the initial temperature, salinity, density and buoyancy frequency profiles shown in Figure 5.

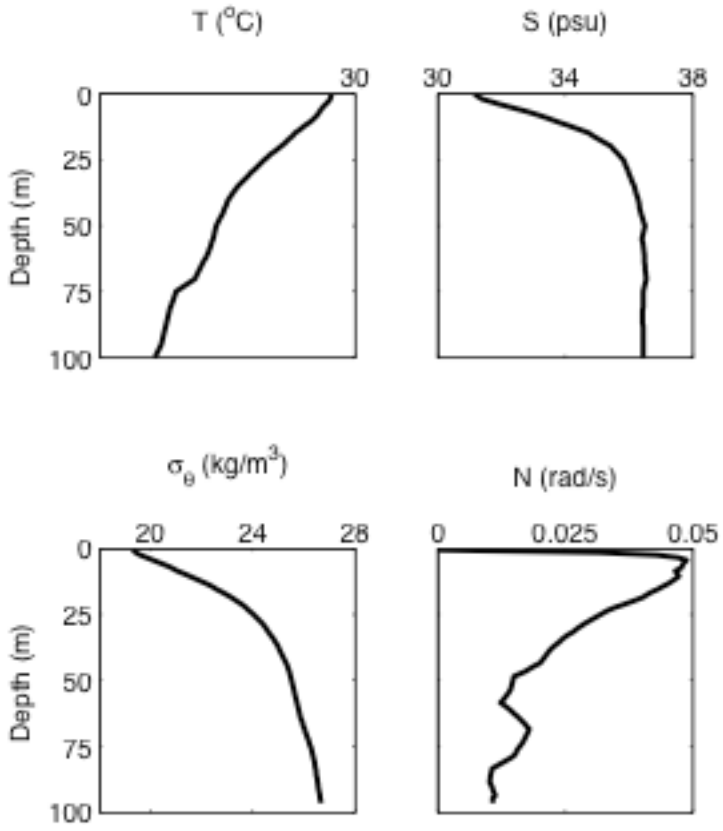

Figure 5. Initial temperature (T), salinity (S), density (σ_θ), and buoyancy frequency (N). These profiles are a smoothed average of observations taken at 12 stations around the Alabama Alps.

A series of simulations of the jet were conducted to create initial conditions to insert into the full GoM domain. The parameters for these simulations are given in Table 2. This resulting initial condition will then be inserted into the results of a GoM simulation that was run to a fully developed state without a jet. All simulations were conducted with the centerline of the jet at mid-depth (50m).

Table 2: Parameters for GoM initialization simulations.

L_x(m)	L_y(m)	L_z (m)	N_x	N_y	N_z	Δx(m)	Δy(m)	Δz(m)	Δt(s)
1024	2048	100	256	512	101	4	4	1	1

The intent of the simulations is to study the interaction of the intermediate and far field of the jet with an ambient IW field, particularly large amplitude, nonlinear internal waves. This prohibits the detailed,

near field modeling of the SSB because at it would require very high resolution in the vicinity of the SSB. Even with grid refinement techniques it is not computationally feasible to simulate both the near and the far field. Thus, the simulation of the SSB starts downstream from the body itself.

It is also desirable to start the simulation before the wake begins to collapse. The onset of wake collapse begins at time $t_c=2\pi/3N$ (Kaulum,1972). At z=50m (where the jet is centered), N=0.0148 rad/s, resulting in t_c =141s.

For these simulations the speed of the SSB, V, is assumed to be 10m/s (~20knots). Thus, the downstream position at the onset of wake collapse is: $x_c=Vt_c$ = 1410m. The downstream starting position of the SSB is arbitrarily set at x=500m, which puts the jet well before the start of the collapse stage, and unstratified relationships can be used to determine the jet maximum velocity and diameter.

For unstratified conditions, Kaulum (1972) provides the following relationship to obtain the wake diameter, D, at doenstream position, x,

$$\frac{D}{D_0} = 1.25\left(\frac{x}{D_0}\right)^n \tag{3}$$

where D_0 is the initial wake diameter and n=0.22 is an empirically obtained exponent. Substituting x=500m into (3) yields a jet diameter D = 29.6m, which is rounded to 30m for these simulations.

A time series of horizontal cross sections of the downstream velocity for the jet simulation in GoM stratification is shown in Figure 6. By hour 2 the jet has penetrated across half the domain and strongly impacts the middle third of the domain. After eight hours the jet extends across the domain. The jet takes up a significant portion of the vertical extent (Figure 7), as it is 30m in diameter vs. 101m domain depth. The jet magnitude decays as it continues to propagate across the domain by hour 10.

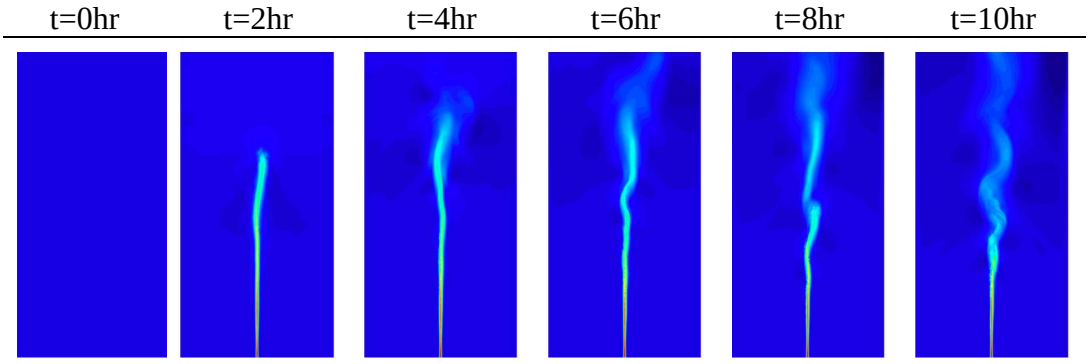

Figure 6. Time series of horizontal cross-sections of V through jet center (z=50m). Color scaling is the same as in Figure 7. The jet progresses into the domain and becomes wavy by t=10hr, reminiscent of a vortex street from the wake of an object.

A horizontal temperature cross section (Figure 8) shows the horizontal variability induced by the jet. Waves are seen on the leading edge and trailing off the front of the jet at an angle. Vortices begin to

form at hour 7 and by hour 10 a von Karman vortex street has formed. Internal waves are forming in the vertical temperature cross section (Figure 9). The waves appear to be significatntly nonlinear and the greatest wave formation is in the center of the domain under the head of the jet. An isosurface of temperature in the horizontal cross section through the center of the jet (Figure 10) clearly shows the creation of nonlinear internal waves in front of and around the jet as well as propagation of the nonlinear internal waves away from the jet.

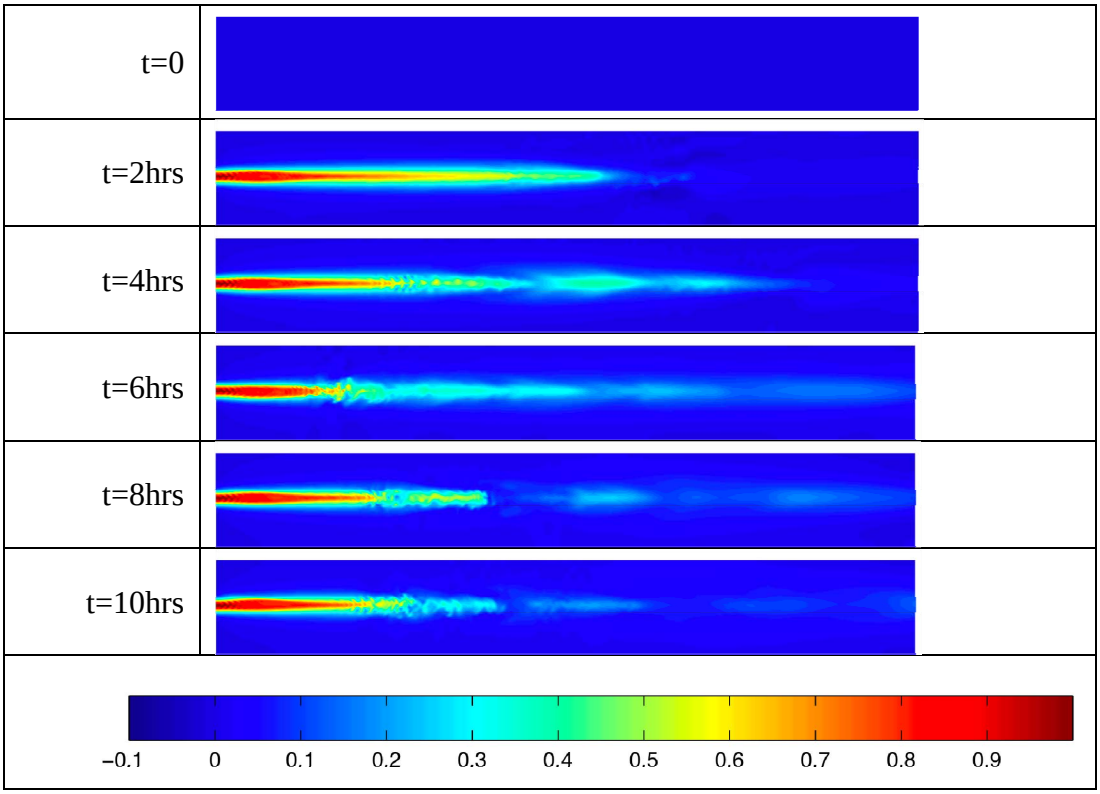

Figure 7. Time series of vertical cross section of downstream velocity, V, through the jet center. Units on color bar are in m/s. The patchiness in the velocity downstream is caused by the oscillation of the jet at it progresses through the simulation domain (Figure 6). Note the jet takes up considerable space as it is 30m in diameter, whereas the vertical extend of the domain is 101m.

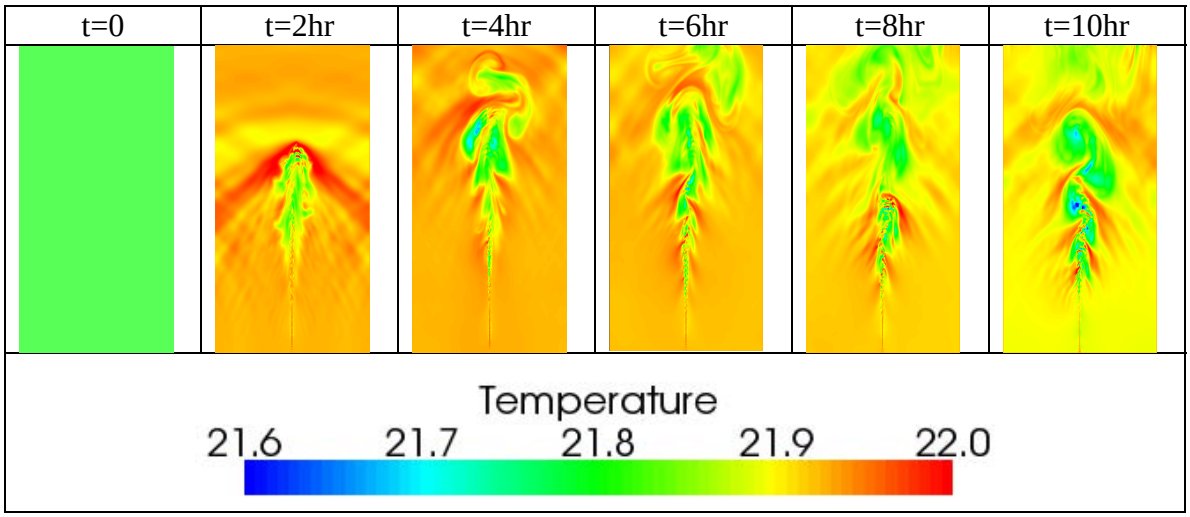

Figure 8. Temperature contours through the center of the jet. A leading wave can be seen in the temperature field at t=2hrs. Also there seems to be a wave generated by the jet that propagates at a near 45 degree angle away from the jet. By t=10 swirls of temperature indicating that a von Karman vortex street has formed.

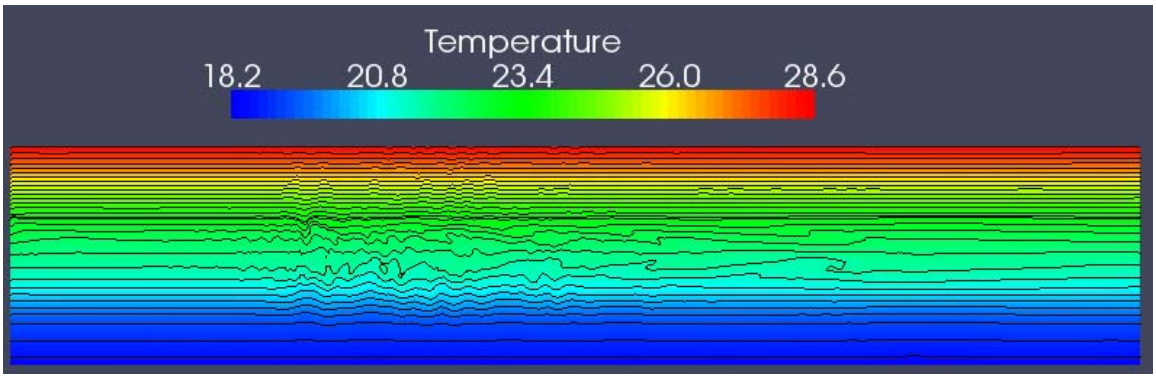

Figure 9. Temperature contours at t=10hrs. The structure seen in the fluctuations near the center of the domain are nonlinear internal waves formed by the jet.

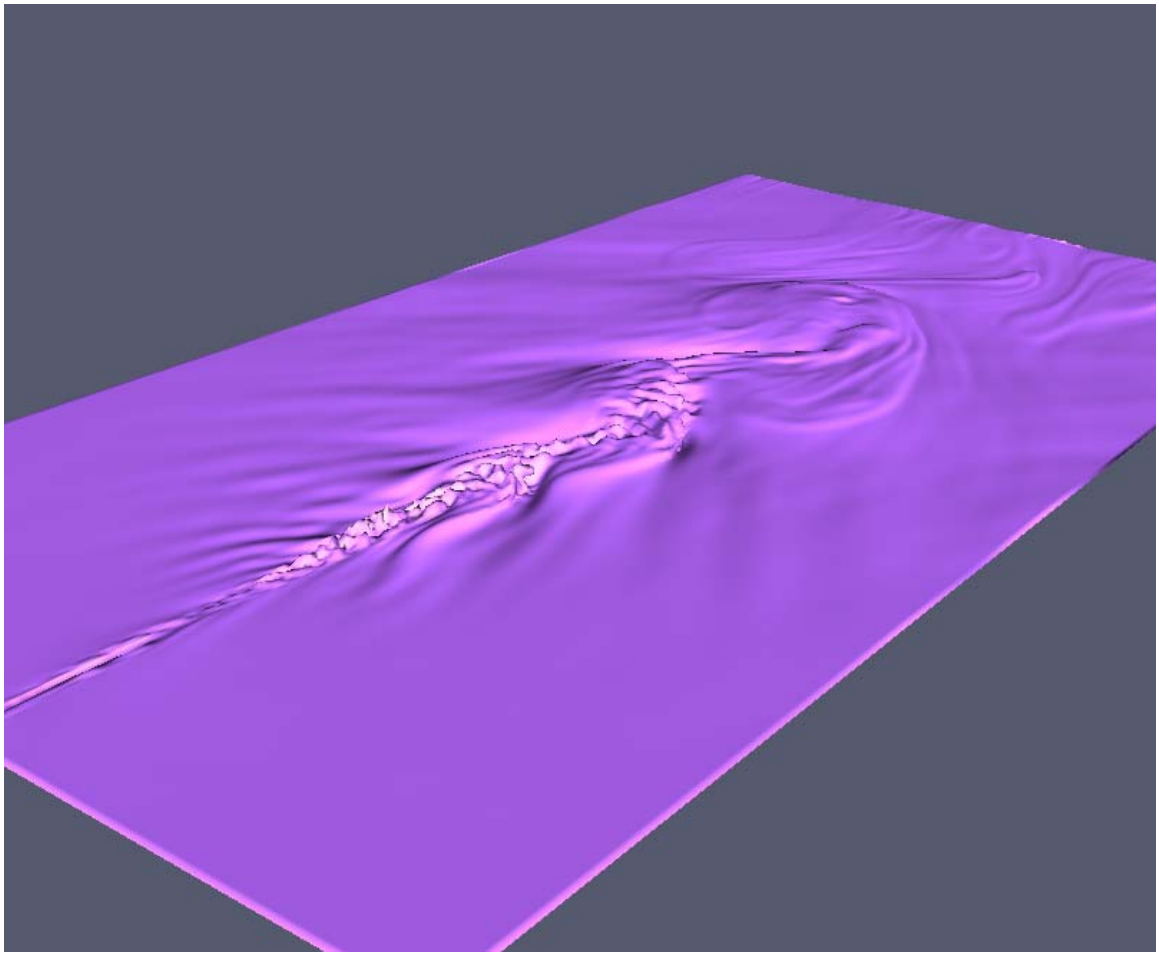

Figure 10. Isosurface of temperature at 10hrs on a horizontal cross section through the centerline of the jet. The jet creates vertical motions that displace temperature. Wave motions can also be seen propagating away from the jet.

Simulations of the flow around the Alabama Alps have been conducted with the temperature and salinity profiles discussed above as initial conditions and a barotropic eastward current as forcing. Experiments were conducted with three forcing speeds, 5 cm/s, 10 cm/s and 50 cm/s. In the 5cm/s case the flow is blocked by the Alps. The flow is hydraulically controlled in the 10 cm/s case and in the 50 cm/s experiment the flow is supercritical, with respect to the Froude number, and nonlinear internal waves form behind the Alps and disperse downstream (Figure 11). This work has been submitted to Geophysical Research Letters (Gallacher, et al., 2008).

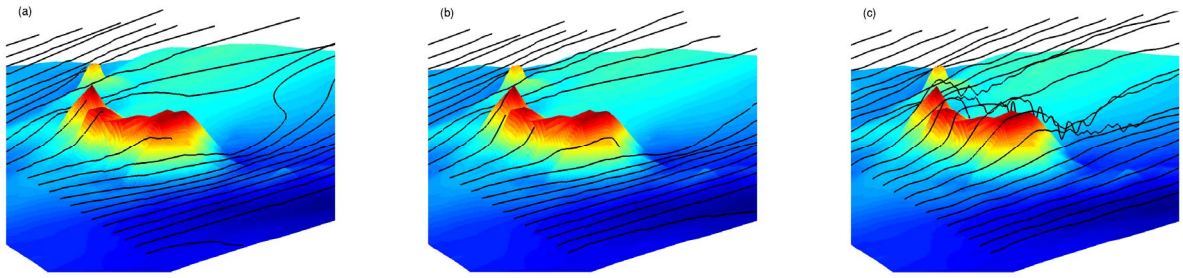

Figure 11: Streamlines for (a) the 5cm/s case; (b) the 10cm/s case and (c) 50cm/s case. Streamlines bend around the alps for the 5 and 10cm/s simulations, indicating flow blocking, whereas the fluid flows over the alps in the 50cm/s simulation.

Although the forcing velocity is consant in time and space, the flow resulting from the interaction with the Alps is quite complex with significant spatial and temporal variability. This can be seen in the kinetic energy dissipation rate shown in Figure 12. Also, the difference in the kinetic energy dissipation rate for the 10 cm/s case versus the 50 cm/s case is substantial.

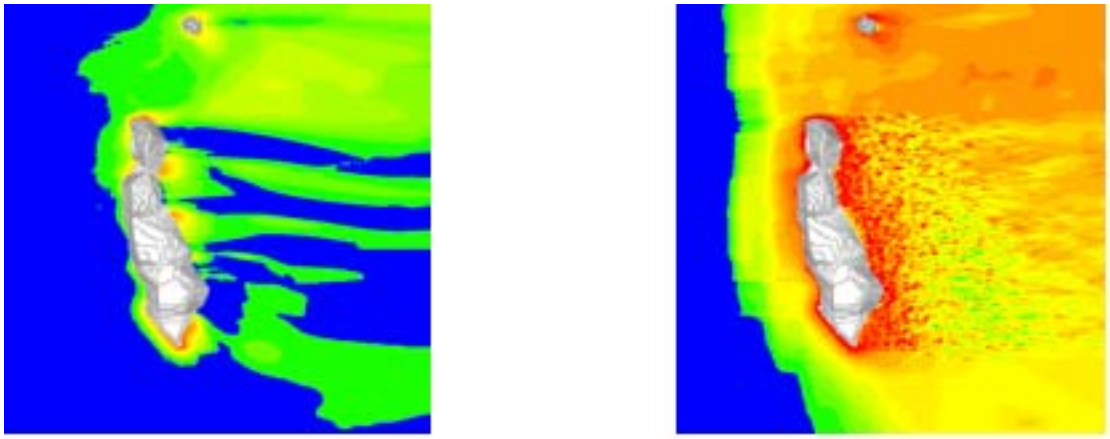

Figure 12. Kinetic energy dissipation rate for U=10cm/s (left) and 50cm/s (right). The 50cm/s simulation is more turbulent and generates a larger wake with more mixing.

IMPACT/APPLICATIONS

This work will help to determine the importance of and the requirements for nonhydrostatic forecast systems for naval applications. The scales and features which will require nonhydrostatic simulation are being assessed.

RELATED PROJECTS

The NRL project Autonomous Characterization of Environmentally Induced Non-Acoustic Noise and the Adaptation of Multi-Sensor USW Networks. (6.2, Undersea Warfare) is related to this project because it involves nonhydrostatic modeling of the SW06 experimental area and time and comparison

with measurements taken during SW06. Components of SW06 are funded through this ONR NLIWI DRI.

REFERENCES

Fadlun, E.A. R. Verzicco, P. Orlandi and J. Mohd-Yusof, 2000. Combined immersed-boundary finite-difference methods for three dimensional complex flow simulations, J. Comp. Phys. 161, 30.

Goldstein D, Handler R, Sirovich L., 1993. Modeling a no-slip flow with an external force field. J. Comp. Phys., 105, 354.

Kaulum, K.W., 1972, "Predictions of Submarine Wake Size and Contaminant Concentrations in an Ocean Environment," DTIC Report A951955

Lai M-C, and C. S. Perskin, 2000. An immersed boundary method with formal second order accuracy and reduced numerical viscosity. J. Comp. Phys., 160, 705.

Lilly, D.K. 1983. "Stratified Turbulence and the Mesoscale Variability of the Atmosphere," J. Atmos. Sci. 40, 749.

Pope, S. B., 2000 *Turbulent Flows*. Cambridge University Press. Cambridge, UK

Riley, J.J. and S.M. de Bruyn Kops, 2003. Dynamics of turbulence strongly influenced by Buoyancy, Phys. Fluids 15, 2047.

Siviente, A. I. & Patel, V. C., 1999. Experiments in the turbulent near wake of an axisymmetric body. AIAA J. 37, 1670–1673.

Tennekes, H and J. L. Lumley. 1972. *A First Course in Turbulence*. MIT Press, Cambridge, MA

Tseng, Y-H and J. H. Ferziger, 2003. A ghost-cell immersed boundary method for flow in complex geometry, Jour. Comp. Phys., 192, 593.

PUBLICATIONS

Gallacher, P. C., D. A. Hebert, M. R. Schaferkotter and Ross T. Landgrave, 2008, Nonhydrostatic Simulations of Hydraulic Control and Internal Waves at a Small Bank on the Continental Shelf, Geophys. Res. Lett. in review.